A Lamb wave based liquid sensor for biomedical applications

Gahar, Widesh; Meyer, Johan; French, Paddy; Sisman, Alper; Korkmaz, Erdal

DOI
10.1109/SSI63222.2024.10740544

Publication date
2024

Document Version
Final published version

Published in
2024 Smart Systems Integration Conference and Exhibition, SSI 2024

2024 Smart Systems Integration Conference and Exhibition (SSI) | 979-8-3503-8877-0/24/$31.00 ©2024 IEEE | DOI: 10.1109/SSI63222.2024.10740544

A Lamb wave based liquid sensor for biomedical applications

Widesh Gahar
Microelectronics - Bioelectronics
Delft University of Technology
Delft, Netherlands
W.A.Gahar@student.tudelft.nl

Johan Meyer
Microelectronics - Bioelectronics
Delft University of Technology
Delft, Netherlands
J.W.D.Meyer@tudelft.nl

Paddy French
Microelectronics - Bioelectronics
Delft University of Technology
Delft, Netherlands
p.j.french@tudelft.nl

Alper Sisman
Microelectronics - Bioelectronics
Delft University of Technology
Delft, Netherlands
sisman@2mel.nl

Erdal Korkmaz
Research Group Smart Sensor Systems
The Hague University of Applied Science
Delft, Netherlands
E.Korkmaz@hhs.nl

***Abstract*— This study presents an AlN based Lamb wave (A0 mode) liquid sensing device that can be used for biomedical applications. The Lamb wave device features a 1.5 µm composite membrane consisting of a 500 nm LPCVD SiN and a 1 µm of a c-axis oriented AlN film. A 45° rotated design was also considered for this project to reduce the reflections from the edges towards the output IDT. A liquid testing experiment involving IPA, DI water, and D-PBS was performed to see if the devices were able to differentiate between these liquids. The results showed that the fabricated Lamb wave devices exhibited sensitivity to mass loading and were able to distinguish between the liquids based on their phase, frequency, and gain characteristics. Notably, devices with the rotated design have shown a substantial increase in resonance by 15 dB, as well as enhanced sensitivity, when compared to the devices with the normal design. Furthermore, the devices featuring the normal design had a Q factor of 450, whereas devices with the rotated design exhibited a Q factor of 680, indicating superior performance of the latter. These findings suggest that a Lamb wave device with the 45° rotated IDT design holds considerable potential for liquid sensing, particularly in biomedical applications.**

Keywords*— *Acoustic wave, AlN, Lamb wave, membrane, SiN

I. INTRODUCTION

The demand for compact, reliable, disposable, and affordable sensors is on the rise in industrial, medical, and various other scientific and engineering sectors. The sensor market is experiencing rapid growth, with an annual increase of approximately 18% [1]. In particular, the biosensor market holds great promise due to its applications in advancing areas of healthcare, biotechnology, and medicine. Areas of medical significance include the utilization of biosensors in personal glucose testing, HIV, and early cancer detection [1].

Acoustic wave based sensors have become an important area of research due to their high sensitivity, compact size and real-time response, which are the main factors for their widespread use. Lamb wave, a type of acoustic wave, can propagate on both side of the plate due to the thin plate structure, enabling both sides to serve as the sensing area. Furthermore, by using the opposite side of the plate (membrane) as the sensing area, the electrodes of the Lamb wave devices can be protected as they will be isolated from the surrounding environment [2]. Lamb waves are excited by the interdigital transducers (IDTs) when the thickness of the substrate is less than or equal to the wavelength of the wave.

Unlike traditional acoustic wave devices where the wave travels solely on the surface, in Lamb wave devices, the entire membrane plate actively participates in the propagation of the acoustic wave. Due to the smaller thickness of the plate compared to the acoustic wavelength, Rayleigh waves are generated on both surfaces of the plate. The overlapping of these waves on the upper and lower surfaces results in the creation of an antisymmetric mode with a lower velocity (or frequency) and a symmetric mode with a higher velocity (or frequency). These modes are commonly referred to as lamb waves [3].

II. DESIGN

A. Lamb wave mode

For Lamb wave devices, the two most useful modes are the lowest order antisymmetric mode A0 and the symmetric mode S0 in plates with a low thickness-to-wave ratio. Lamb wave velocities of A0 and S0 modes can be determined with the following equations:

$$V_{A0} = \frac{2\pi h}{\lambda}\sqrt{\frac{E}{12(1-v^2)p}}\frac{1}{\sqrt{\frac{\pi^2 h^2}{3\lambda^2}+1}} \quad (1)$$

$$V_{S0} = \sqrt{\frac{E}{(1-v^2)p}} \quad (2)$$

where E = Young's modulus, v = Poisson's ratio, ρ = density, h = thickness, and λ = wavelength of Lamb wave. On ultra-thin plates, the Lamb wave velocity in S0 mode is dispersionless and does not depend on the plate thickness, whereas the wave velocity in A0 mode does depend on the plate thickness [2]. The resonant frequency of a Lamb wave device is determined by:

$$f_0 = \frac{V_p}{\lambda} \quad (3)$$

where $V_p = V_{A0}$ or $V_p = V_{S0}$.

The A0 mode, also referred to as flexural plate wave (FPW), exhibits a high sensitivity to mass loading and can effectively be employed in liquid environments with minimal attenuation [4]. Therefore, the A0 Lamb wave mode will be employed in this study.

B. Material selection

The base substrate chosen for this project was a 4” p-type Double Side Polished (DSP) Si wafer with (100). Additionally, AlN was selected as the piezoelectric material. The electromechanical coupling coefficient has the highest value along the (002) orientation[5]. Therefore, the aim of this project was to produce a high quality (002) oriented 1 um of AlN layer to serve as the piezoelectric layer for the Lamb wave device. The use of Interdigital Transducers (IDT) is the most direct and effective method of exciting surface acoustic waves on a piezoelectric substrate. Gold was used as the material for the electrodes. To ensure proper adhesion of the gold layer onto the piezoelectric layer, a thin layer of chromium needed to be deposited first. Finally, a high quality SiN layer was needed on the backside of the wafer to create the patterned etch mask for the wet etching process. A high quality SiN layer below the piezoelectric layer was also necessary to act as an etch stop layer during the KOH wet etching process [6]. Hence, the LPCVD technique was employed to ensure the deposition of high-quality SiN layers on both sides of the wafer.

C. IDT design

The two-port structure, also known as the bidirectional IDT structure, consists of an input and output port, was used in this study. Fig. *1* illustrates the standard bidirectional IDT structure, which encompasses four key factors: width, number of finger pairs, aperture (overlap of fingers), and the length of the delay line[7]. Three different delay line lengths will be utilized for this project. The IDT design parameters are placed in table 1.

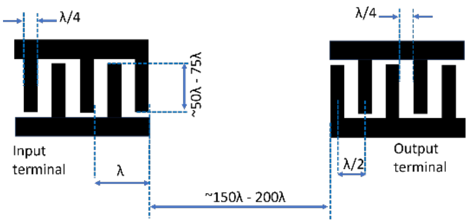

Fig. 1. IDT design.

TABLE I. IDT DESIGN PARAMETERS FOR THE LAMB WAVE DEVICE

IDT DESIGN PARAMETERS	Device		
	1	*2*	*3*
Finger width (μm)	5	5	5
Wavelength (μm)	20	20	20
Number of Finger pairs	30	30	30
Aperture (λ)	75	75	75
Delay line length (μm)	750	1000	1500
Thickness (Cr/Au) (nm)	100	100	100

Reflections from edges towards output IDT

When the waves of the Lamb wave device is generated by the left-side (input) IDT and received by the right-side (output) IDT, some of the wave energy will be reflected back from the silicon substrate to the output IDT. In order to reduce the reflection from the edges towards the output, a 45◦ rotated bidirectional IDT design was also considered to see if the reflections can be reduced. The initial IDT design and the modified IDT design can be seen in Fig. *2*. The arrows in the figures illustrate the directions of the reflected waves.

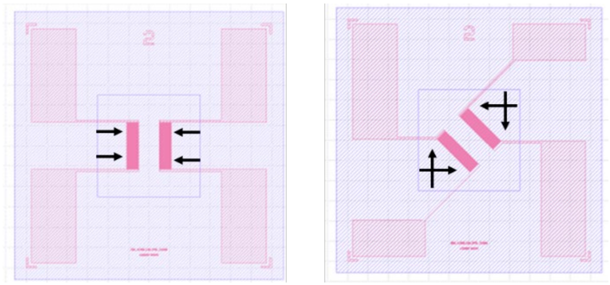

Fig. 2. (a) Design 1 – Normal (b) Design 2 - Rotated

III. COMSOL SIMULATION

A 3D block study was performed using COMSOL with the desired membrane layers in order to find the resonant frequency of the device. The design consists of 500 nm SiN as the bottom layer, 1 μm AlN (piezoelectric layer) and on top 100 nm of Au electrodes (IDTs).

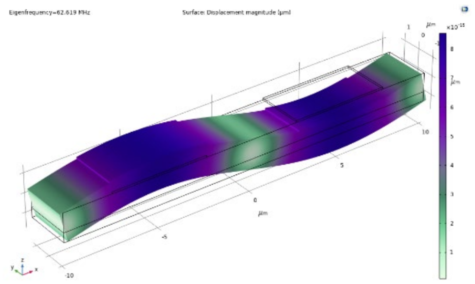

Fig. 3. Eigenfrequency study.

Fig. *3* shows the result after performing an eigenfrequency study to find the resonant frequency of the device. A clear A0 mode was observed at around 63 MHz. The resonant frequency of the A0 Lamb wave device was also determined by utilizing equations 1 and 3. This confirms that the resonant frequency of the designed A0 Lamb wave device is 63 MHz.

IV. FABRICATION

The main processing steps for the fabrication of the Lamb wave devices are shown in Fig. *4*.

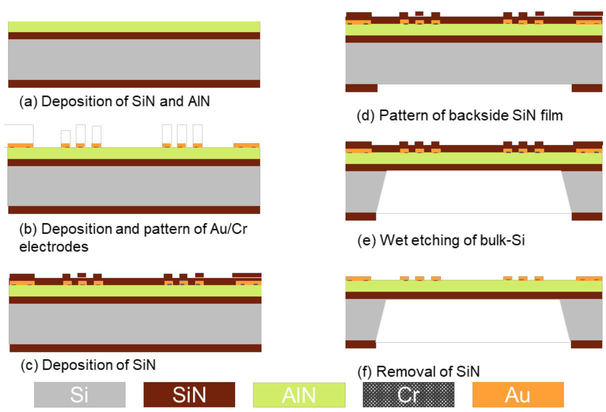

Fig 4. Main fabrication steps for the Lamb wave devices.

V. EXPERIMENTS

On a printed circuit board (PCB), two devices were attached: one with the normal IDT design and another with the rotated IDT design, both having the same delay line length. Fig. *5* shows the overview of the Lamb wave devices attached on a PCB and ready for measurements.

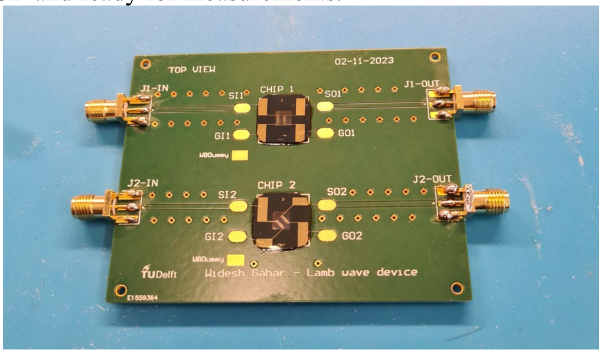

Fig. 5. Lamb wave devices attached and wirebonded on a PCB with the SMA connectors.

Testing was performed by measuring the S21 parameter between 10 kHz and 100 MHz with the help of a Vector Network Analyzer. The liquids that were used for the liquid testing experiments were: IPA (Isopropyl alcohol), DI water and D-PBS (Dulbecco's Phosphate-Buffered Saline). The experiment involved placing a volume of 40 µL of the selected liquids on the sensing area of the device.

VI. (EXPERIMENTAL) RESULTS AND DISCUSSION

The phase and gain plots achieved from the S21 parameter measurements for device 2 are presented in the figures below. Differences in frequency, phase and gain are observed across different liquids, implying that the produced devices exhibit sensitivity towards mass loading and can differentiate between various liquid substances. Furthermore, the length of the delay line does not significantly impact the outcome. These observations remain valid even for devices with the rotated design.

A. S21 Gain

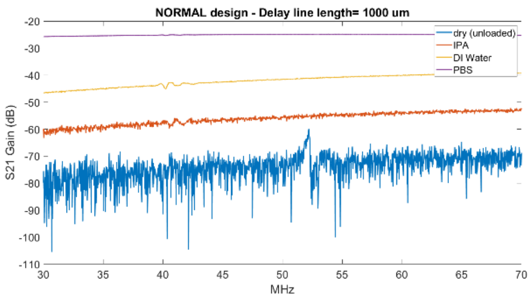

Fig. 6. Device 2 Gain comparison - NORMAL design.

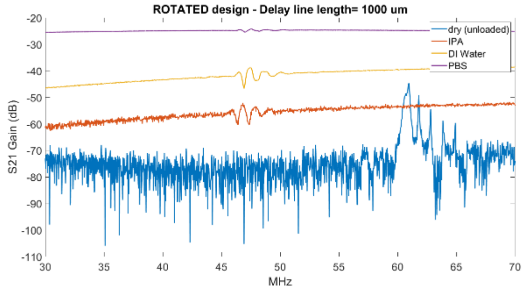

Fig. 7. Device 2 Gain comparison - ROTATED design.

B. S21 Phase

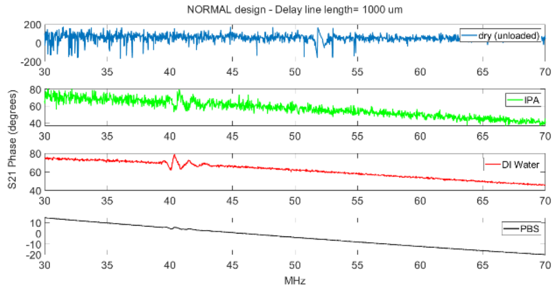

Fig.8. Device 2 Phase comparison - NORMAL design.

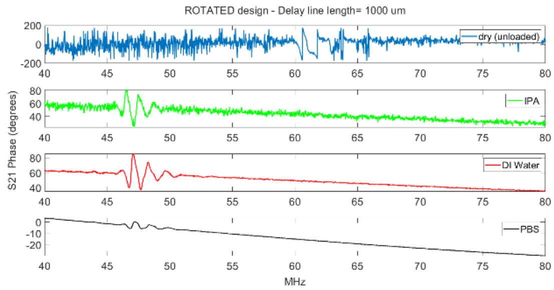

Fig. 9. Device 2 Phase comparison - ROTATED design.

C. Phase shift vs density

The relationship between the phase shift and the density of the liquid for the devices with the normal and rotated design is presented in *Fig 10*. Normal design devices exhibit an average 80-degree phase shift with IPA, while rotated design devices show 81 degrees. The phase shift difference between IPA and DI water is 2 degrees for normal design and 13 degrees for rotated design. Due to the faster evaporation rate of IPA in comparison to other liquids, the volume of IPA does not remain constant, thereby hindering accurate comparisons with the other liquids. Nonetheless, there are noticeable variations in the gain of IPA and DI water. The phase shift difference between D-PBS and DI water is 72 degrees for normal design and 92 degrees for rotated design, favouring the latter for superior performance.

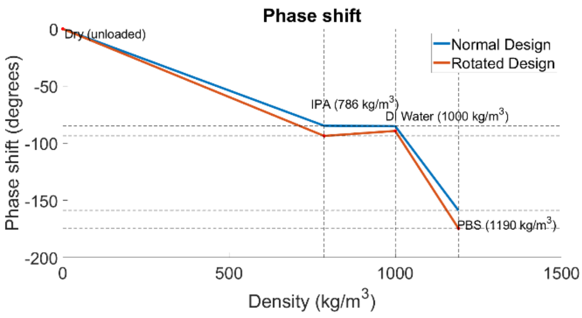

Fig. 10. Phase shift vs liquid density

D. Frequency shift vs density

The graphs illustrating the relationship between frequency shift and density for both designs are provided below. Adding IPA to the sensing area results in an average frequency shift of 11 MHz for devices with the normal design, and an average frequency shift of 13 MHz for devices with the rotated design as seen in *Fig. 11*. The average frequency difference between IPA and DI water for the normal and rotated design devices is 430 kHz and 450 kHz, respectively. Furthermore, the average frequency difference between DI water and D-PBS is 90 kHz for normal design devices and 100 kHz for rotated design devices. Also here, the rotated devices do show a better shift between the liquids, indicating that they are more sensitive.

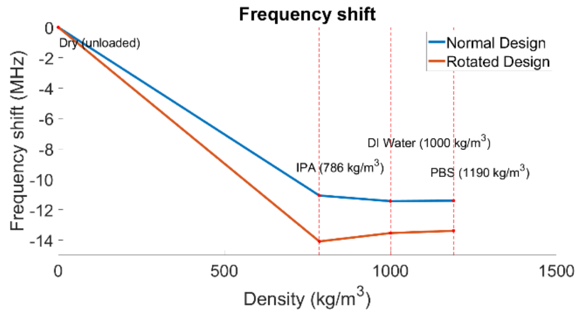

Fig.11. Frequency shift vs liquid density

E. Analyzing performance parameters for devices with Normal and Rotated designs

The devices with the normal design have an average Q factor of 450, while the devices with the rotated design have an average Q factor of 680. The gain comparison between the normal and rotated IDT design for Device 2 is depicted in Fig. *12.* A noticeable difference can be observed in the resonance of the device equipped with the rotated IDT design, which outperforms the device featuring the normal IDT design by 15 dB.

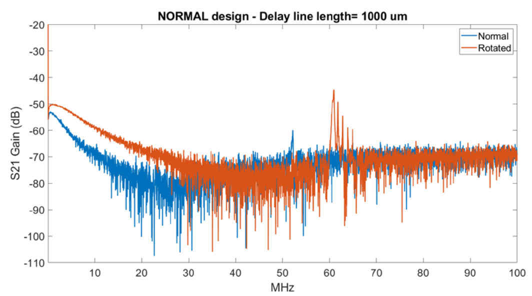

Fig. 12. Gain comparison between Normal and Rotated design for Device 2.

VII. Conclusion

The fabricated devices were capable of generating the A0 Lamb wave mode, which was detected through the use of a Vector Network Analyzer. Despite simulations predicting a resonant frequency of 63 MHz, actual devices showed discrepancies. Normal IDT design devices resonated at 52 MHz, while rotated design ones at 60 MHz due to thinner AlN deposition than desired. Various liquids (IPA, DI water, D-PBS) were tested, revealing differences in phase, frequency, and gain shifts. Rotated design devices demonstrated higher sensitivity, better resonance, with larger frequency and phase shifts, and an average Q factor of 680 compared to 450 for normal design devices, attributed to reduced reflections. Therefore, for liquid sensing applications, the rotated design is recommended over the normal design.

Acknowledgments

This project would not have been possible without the people who supported me every step of the way. I would also like to express my sincere appreciation to the dedicated staff at Else Kooi Lab and Kavli Nanolab for their pivotal involvement in the successful fabrication of the devices.

References

[1] N. Gözde Durmuş et al. "Acoustic-Based Biosensors". In: Encyclopedia of Microfluidics and Nanofluidics. Springer US, 2014, pp. 1–15. ISBN: 9783642277580. DOI: 10.1007/978-3-642- 27758-0_10-2. URL: http://dx.doi.org/10.1007/978-3-642-27758-0_10-2.

[2] Mengwei Liu et al. "Design and fabrication of a MEMS Lamb wave device based on ZnO thin film". In: Journal of Semiconductors 32.4 (Apr. 2011), p. 044006. DOI: 10.1088/1674-4926/32/ 4/044006. URL: https://doi.org/10.1088/1674-4926/32/4/044006

[3] Lokesh Rana et al. "Development of MEMS-based Lamb Wave Acoustic Devices". In: IEEE Trans- actions on Electron Devices 65.4 (2018), pp. 1523–1528. DOI: 10.1109/ted.2018.2805698.

[4] R. Duhamel et al. "Sensitivity of a Lamb wave sensor with 2μm AlN membrane". In: Ultrasonics 44 (Dec. 2006), e893–e897. ISSN: 0041-624X. DOI: 10.1016/j.ultras.2006.05.206. URL: http://dx.doi.org/10.1016/j.ultras.2006.05.206.

[5] Abid Iqbal and Faisal Mohd-Yasin. "Reactive Sputtering of Aluminum Nitride (002) Thin Films for Piezoelectric Applications: A Review". In: Sensors 18.6 (June 2018), p. 1797. ISSN: 1424-8220. DOI: 10.3390/s18061797. URL: http://dx.doi.org/10.3390/s18061797.

[6] Fatemeh Gholami et al. "A study of optimizing lamb wave acoustic mass sensors' performance through adjustment of the transduction electrode metallization ratio". In: Sensors 22.17 (2022),p. 6428. DOI: 10.3390/s22176428.

[7] Zhenzhen Chen et al. "Acoustic microreactors for chemical engineering". In: Chemical Engineer- ing Journal 433 (Apr. 2022), p. 133258. ISSN: 1385-8947. DOI: 10.1016/j.cej.2021.133258. URL: http://dx.doi.org/10.1016/j.cej.2021.133258